EUROPEAN FUSION DEVELOPMENT AGREEMENT

EFDA–JET–PR (01)69

S.K. Sipilä et al

Recent Developments in Monte Carlo Codes for Edge Plasma Studies

Recent Developments in Monte Carlo Codes for Edge Plasma Studies

[1]S.K. Sipilä, [2]J.A. Heikkinen, [1]T.P. Kiviniemi,
[1]T. Kurki-Suonio, [3]W. Fundamenski, [4]K. Nordlund

[1]Helsinki University of Technology, Advanced Energy Systems,
Euratom-Tekes Association, P.O. Box 2200, FIN-02015 HUT, Finland
[2]VTT Chemical Technology, Euratom-Tekes Association, P.O. Box 1404, FIN-02044 VTT, Finland
[3]UKAEA/Euratom Fusion Association, Culham Science Centre, Oxon OX14 3DB, U.K.
[4]Accelerator Laboratory, P.O. Box 43, FIN-00014 University of Helsinki, Finland

e-mail: Seppo.Sipila@hut.fi

Preprint of the Paper to be published in the Proceedings of 8th Int. Workshop on Plasma Edge Theory in Fusion (Sept 2001)

ABSTRACT

In recent years, the rapid evolution of computing power, available computer memory and parallel processing methods have brought the self-consistent modelling of edge plasmas in fusion devices within reach. The use of orbit-following Monte Carlo simulation has been validated in numerous challenging problems of neoclassical physics, and molecular dynamics simulations of plasma wall interactions can be utilized to obtain impurity yields for use in edge plasma and neutral codes. A combination of such methods may facilitate the self-consistent description of edge plasma transport in fusion devices.

1. INTRODUCTION

In describing the tokamak edge plasma, models are needed for the transport of both plasma particles and neutral gas. The line radiation emitted in electron-ion and electron-neutral collisions, the recombination of plasma to neutrals, the plasma and the neutrals are tightly coupled, and their effects must be included self-consistently. Various two-dimensional plasma transport codes, B2 [1, 2], EDGE-2D [3], UEDGE [4], PLANET [5], and UEDA [6], model transport in the poloidal plane assuming uniformity in the toroidal direction. In all these codes, fluid equations are used and the transport equations are discretized by the finite volume method. The neutral transport is treated either by a Monte Carlo (MC) code or by a reduced Navier-Stokes fluid model. Monte Carlo neutral codes such as EIRENE [7], DEGAS 2 [8] and NIMBUS [9] are used in B2 and EDGE-2D. These MC codes solve a kinetic equation for the neutral particle distribution function and treat in detail plasma-surface interactions such as adsorption, reflection and thermal emission, physical sputtering, and chemical erosion. Proper averages of the neutral distribution provide the plasma source or sink terms, which are coupled back to the plasma code. Usually, the neutral distribution is assumed to change slower than that of the plasma, justifying the use of a coarser time grid or subcycling in the Monte Carlo code. Models of physical and chemical sputtering of varying degrees of sophistication are included, and both atoms and molecules are simulated. The two coordinates (poloidal and radial) are usually orthogonal, except in regions near divertor targets where the mesh is distorted to fit their actual shape. The flux surface mesh is obtained from the actual MHD equilibria (e.g. from the EFIT Code).

Monte Carlo treatment of neutrals can be regarded as a necessity whenever long neutral trajectories exist (e.g., in regions of low plasma density). A comparison of fluid and Monte Carlo neutral transport codes in slab geometry has shown that the power at which the transition between attached and detached divertor plasma occurs agrees to within 30% in these models [10]. It should be noted that the simulations require the determination of several input parameters that are not well known experimentally, such as the anomalous transport coeffcients at the plasma edge, the effective pumping rate of the plasma facing components, and the fraction of the target ion current that recycles as neutrals. Either Bohm transport or spatially constant diffusivities are assumed for the anomalous transport coefficients. In Monte Carlo codes, geometric details such as the shape of the targets can be accurately treated. In fluid models, however, these must be introduced as various boundary conditions.

Separate Monte Carlo modelling of the particle bombardment of idealized solids including surface roughness have been performed to evaluate statistical estimates for the surface reflection coefficients of particle, energy, and momentum fluxes for most target-projectile combinations. Non-reflected incident ions and atoms are assumed to be absorbed and subsequently re-emitted as thermal molecules, and all incident molecules are adsorbed and re-emitted without reflection, provided the surfaces are saturated (e.g., the divertor targets). The physical sputtering yield in all models is given by the empirical Eckstein-Bohdansky fit, and the energy spectrum of emitted particles is assumed to be given by a Thompson distribution [11]. For chemical sputtering, a simplified model where one introduces the neutral carbon as an atom with 1eV energy results in good agreement with the more complete model. Various databases exist for the rate coefficients for charge exchange, ionization, recombination, and for the associated energy exchange for the latter, and these rates are reviewed in Ref. [12].

The described hybrid fluid-Monte Carlo codes for the simulation of SOL and divertor plasmas are used routinely for ASDEX-Upgrade (B2-EIRENE), for the JET experiment (EDGE2D-NIMBUS), and for DIII-D (fully fluid-based model in UEDGE). An extensive review of the validation of fluid-Monte Carlo edge codes for impurity production and transport, helium, neon, and nitrogen seeded discharges, discharges with carbon, physics of detachment, ion flux profiles, divertor geometry effects, and various time dependent phenomena like ELMs is provided in Ref. [13]. The codes have been used to fit experimental profiles upstream and at the divertor targets, and reasonable agreement (factor of two) with available data on impurity transport has been obtained. The codes have successfully modelled transient events such as type I and type III ELMs, and have been able to follow MARFE formation into the core of the plasma. The detailed crossfield profiles of particle flux to the divertor targets seem to require a more sophisticated (kinetic) treatment of the plasma. Also, the possible role of molecular activated recombination is an active area of investigation. Opacity and kinetic effects including various drifts are not generally included, and neutral-neutral collisions are not used in Monte Carlo codes. E x B and ∇T x B drifts are incorporated in UEDGE and a special version of B2, but the use of these terms seriously slows down the codes, and their quantitative impact on the solutions needs investigation.

With the advent of computing environments with large memory capacity and massively parallel processing, replacement of the fluid-like plasma transport part in the above-mentioned edge codes by a Monte Carlo plasma particle code has become a realistic alternative. The progress in the development of gyrokinetic particle-in-cell codes [14] for turbulent plasma simulation and in the validation of standard Orbit-Following Monte Carlo (OFMC) codes for the neoclassical plasma simulation around the separatrix in actual geometry [15] show the competence of the Monte Carlo approach in edge simulation. Moreover, two-dimensional electrostatic particle-in-cell codes have been used to validate various physical concepts of sheath formation in the SOL magnetic surfaces linking the divertor targets. Presently, using subcycling for the electron part of the distribution, time steps of the order of 10^{-7}s for advancing the ion distribution in a 20 cm wide layer around the

separatrix, including the true divertor geometry for a JET-sized device, require a few hours of CPU time in a non-parallel run for a neoclassical plasma up to one millisecond time period. Therefore, with parallel processing realistic simulations can be performed up to the period of ELMs (tens of milliseconds) or to achieve steady-state in the SOL flows. By proper treatment of the boundaries and replenishment of the wall-adsorbed plasma particles, turbulence driven transport could be simulated by first principles across the separatrix together with the generation of the SOL flows. Here, obviously, consideration of electromagnetic field fluctuations [16,17] are required which have so far not been routinely modelled in gyrokinetic codes. Combination of such codes with the Monte Carlo neutral transport codes can be regarded as feasible, but has not been tried so far. Also of interest are the prospects of using molecular-dynamic simulations to establish the proper boundary conditions, e.g., the coefficients for reflection as well as physical and chemical sputtering. In the following, various validation examples of orbit-following Monte Carlo plasma transport simulation for edge/SOL plasma analysis are described. The guiding-centre orbit-following Monte Carlo code ASCOT has been used to analyse the behaviour of edge plasma ions under the combined influence of a radial electric field, guiding-centre drifts, collisions, and orbit losses. Also, a description and status of molecular-dynamic simulation methods for the divertor target surfaces is given.

2. SIMULATING THE RADIAL ELECTRIC FIELD, ION LOSS AND DRIFTS

The automatic ambipolarity of the radial electric field Er does not hold, e.g., in the presence of a biased internal electrode, ion orbit loss current, or other sources or sinks of toroidal momentum. In that case, two different approaches can be chosen: First, the particle flux in response to a fixed and maintained Er can be calculated, or, second, the ambipolar Er maintaining the radial current balance can be solved. The knowledge gained from the first approach can be used in current balance analysis, but since many different current components indeed consist of the same current carriers, only the self-consistent simulation of all these can give reliable results. This can be done by evaluating the net radial motion of the test particle ensemble in the presence of collisions and guiding-centre drifts in a real tokamak geometry and solving the time change of Er from the polarization equation until the ion flux vanishes. This method has been recently included in the ASCOT code. The solution method is introduced in subsection 2.1 and some results obtained with the method are reviewed in subsection 2.2.

2.1 NUMERICAL METHOD

The initialization of the ion ensemble is done according to the assumed background density and temperature. The weight factors assigned to the test particles are proportional to the total particle number contained in the initialization volumes, and thus reflect the density profile. The particles are distributed randomly in velocity according to a Maxwellian distribution that corresponds to the local temperature. The magnetic background is assumed stationary. The guiding-centre orbits of the test ions are followed in tokamak geometry. In modelling ion-ion collisions, the momentum and

energy conserving binary collision model [18] is used. The code has been routinely used in solving neoclassical fluxes and flow velocity components from the collective motion of the test particles in the presence of binary collisions. For fixed Er, the adopted numerical model has been recently tested in Refs. [19, 20] by calculating poloidal rotation relaxation rates for a homogeneous plasma, and by comparing with the analytic expressions the perpendicular conductivity and parallel viscosity evaluated by ASCOT. If the radial electric field is left to develop, it can be solved self-consistently from the collective motion of the test particles using the polarization equation

$$\frac{\partial E_r}{\partial t} = -\frac{1}{\varepsilon_\perp \varepsilon_0} \langle j_r - j_{pol} \rangle \qquad (1)$$

where j_{pol} and j_r are the radial components of the polarization current and the total current, respectively, and $\varepsilon_\perp \approx \langle n_i m_i, \nabla\rho/\varepsilon_0 B^2 \rangle / \langle \nabla\rho \rangle$ is the perpendicular dielectric constant. Here, subscript i refers to ions, ρ is the flux surface label, and $\langle .... \rangle$ denotes the flux surface average. Assuming that turbulence is ambipolar and that electrons provide a stationary background, the radial current can be written as;

$$j_r(\rho, \theta) = j_c + j_{pol} + j_{visc} + j_{cx} + I_E = A(\rho)$$

in which j_c is the neoclassical radial ion current arising from standard guiding-centre drifts in the presence of ion-ion collisions including also the effect of ion orbit losses, but excluding the polarization current j_{pol} which is here written separately. The current component j_c can be solved by ASCOT. Also the gyroviscosity current, j_{visc}, which is not a genuine guiding-centre drift, is included in j_r, as well as the current due to CX collisions with neutrals, j_{cx}. If probe experiments are simulated, also the electrode current I_E running in the electrode shaft has to be included in the current balance. Here, $A(\rho)$ is the area of the magnetic surface at ρ. A steady-state is found by extending the calculation over several bounce periods and collision times. A more detailed description of the method including benchmark tests, initialization and boundary conditions, is given in [15, 21].

2.2 THE RADIAL ELECTRIC FIELD

In a series of ASCOT simulations [22, 21], the plasma temperature, density, and toroidal magnetic field have been varied over a wide parameter range of ASDEX Upgrade and JET data using typical parameters at L-H transition conditions of each device. However, a clear effect is only found when changing the temperature. An example of this is shown in Fig.1(a), where JET parameters are used and the temperature is varied around L-H transition conditions. The E xB shear increases approximately linearly as a function of temperature (the gradient length is here kept constant). Using Hahm-Burrell shearing rate [23] the shear values of the Er profiles have been analyzed and the parametric dependence $w_{ExB} \propto T^{1:1} n^{0:1} B_t^{-0:85} [s^{-1}]$ for ASDEX Upgrade and JET was obtained from data for the shear. In Refs. [22, 21] the obtained shear values were compared to the BDT criterion and a rough qualitative agreement was found for the simulated shear at threshold conditions

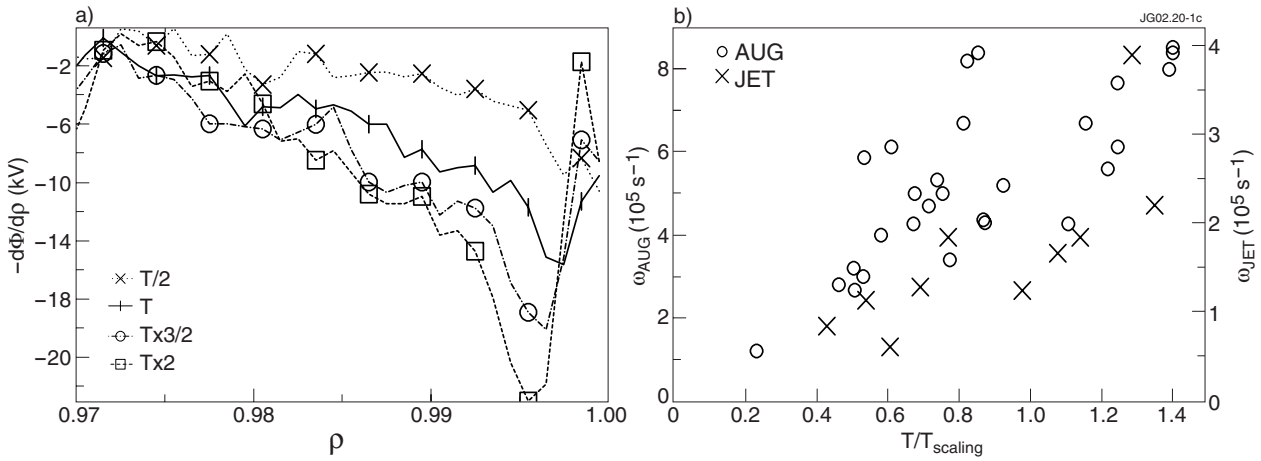

Fig. 1: (a) -dΦ=dρ as a function of radius for plasma temperatures varied around the L-H transition conditions at JET. (b) the Hahm-Burrell shearing rate $\omega_{E\times B}$ from ASCOT simulation as a function of temperature normalized to the experimental L-H transition threshold temperature in ASDEX Upgrade (AUG) and JET.

and the critical shear. However, simulations indicated that the critical shear should be lower for JET than forASDEX Upgrade. This same result is shown in Fig.1(b), where the shear values from the simulation are plotted as a function of temperature which is normalized to the threshold temperature of each device (note the different scale of the vertical axis). In these simulations, no bifurcation was found. A similar simulation for the limiter device TEXTOR was done in Ref. [24, 22], including also the current due to neutral friction as well as the electrode current. There a bifurcation and a solitary-structured Er were found. The effect of ripple diffusion on Er was studied in Ref. [25] with the present method, but its effect was found insignificant. Although the particle flux due to ion-ion collisions vanishes in the presence of ambipolar Er, the simulation of heat flux is still possible. Simulation of ion heat flux has been carried out with ASCOT in Ref. [26] at a transport barrier where the analytic theory is not valid.

2.3 PARTICLE DIAGNOSTICS ISSUES

It has been suggested [27] and further confirmed by ASCOT simulations [28] that the underlying reason for the experimentally observed increase in the neutral particle flux from ripple-trapped slowing-down neutral beam ions at L-H transition is connected with the establishment of a radial electric field Er: when the (negative) radial electric field is large enough in relation to the particle energy, it can confine the particles, trapped in the toroidal ripple, that would otherwise be promptly lost [29]. Therefore, Neutral Particle Analyzers (NPA) could provide a fast and simple means of diagnosing edge Er.

ASCOT has been used in simulating neutral beam ions both with and without an externally imposed radial electric field. A detailed NPA simulation model has been implemented in ASCOT [30], and a simplified version of it has been successfully applied in studying the detection of the radial electric field using NPA on ASDEX Upgrade [28], DIII-D [31] and FT-2 tokamaks [32].

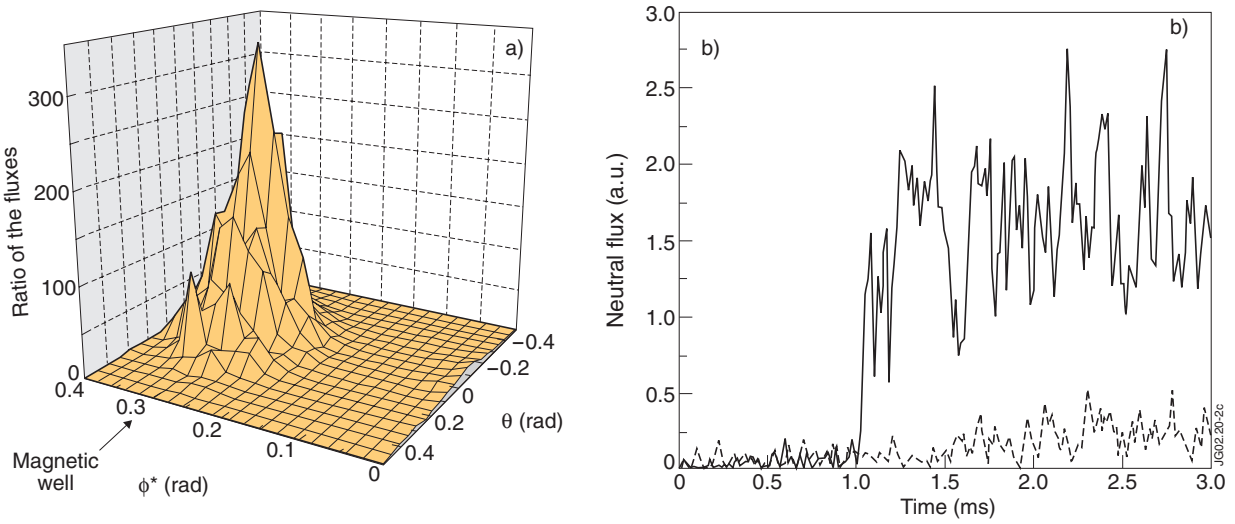

Fig. 2: (a) Ratio of neutral flux with E_r to that without E_r vs. toroidal (∅) and poloidal (θ) angle. (b) time evolution of the neutral flux in response to an abrupt onset of the radial electric field at time t = 1 ms.

Figure 2(a) shows the simulation results as the ratio of the neutral particle flux in the presence of a radial electric field to the flux in the absence of such a field as a function of toroidal and poloidal angle in the plasma edge region. The signal is collected on a 20 x 20 grid that maps the region of interest. Clearly, the ions that are most sensitive to the radial electric field reside in the ripple-trapped part of the phase space. According to the simulation, the presence of a radial electric field can be best observed by monitoring ions near the bottom of the ripple well, for poloidal angles slightly below the mid-plane.

Figure 2(b) shows the time evolution of the neutral flux in response to an abrupt onset of the radial electric field at time t = 1 ms. The simulation is started well before the onset of the field to obtain stationary conditions, and new beam ions are steadily introduced throughout the simulation. For comparison, also the time evolution in the absence of a radial electric field is shown (dotted line). Before the radial electric field is turned on, only a weak signal is observed but, at t = 1 ms, a fast growth is observed in the simulation where the radial electric field is turned on at this time, while the curve corresponding to the case without a radial electric field remains at its low level. Constrained by the statistical accuracy of the simulation, the signal growth can be characterized by a response time of about 50 μs to the field onset.

In an ongoing study the possibility of using the low-energy channels of CX detectors in ASDEX Upgrade to determine the edge ion temperature (T_i) profile is investigated. The method is based on the fact that the coupling of the plasma ions to the local neutrals via charge exchange is particularly strong in the edge plasma where the plasmatemperature is reasonably low and the neutral density is high. Consequently, the energy spectrum of the neutral fluxes measured by the neutral particle analysers contains the information about the ion temperature profile. In this method an ‘ad-hoc’ ion temperature profile, specified as a linear spline, is combined with the other profiles to calculate the neutral fluxes. However, with very steep temperature pedestals in the plasma edge, it is not clear if a local temperature can be used to characterize the plasma. With ASCOT, the simulated local ion temperature profile (extracted from the perpendicular velocity distribution of

the test particles) has been found to reflect well the true temperature for weak temperature gradients at the edge, but for very steep gradients the particle distribution begins to display non-Maxwellian features [33].

3. SIMULATION OF DIVERTOR TARGET LOAD ASYMMETRIES IN JET

Extending the lifetime of the divertor targets is a key question in the design and operation of ITER, and will also be of great concern in JET under the Enhanced Performance operation. In JET, measurements of the heat loads to the divertor targets have shown that the load to the outer target displays a few mm wide peak close tothe separatrix. Such a 'hot spot' structure can substantially diminish the lifetime of

divertor targets. Furthermore, a strong asymmetry is observed between the inner and outer targets, and the ions seem to dominate the load at least in H-mode conditions [34]. Because sharp load peaks near the separatrix suggest the involvement of the direct orbit loss mechanism, a detailed study of the kinetic behaviour of the ion component in the vicinity of the separatrix is necessary. The H-mode divertor load distributions in JET have been simulated with ASCOT using experimental magnetic background, density and temperature profiles as well as wall and divertor location data together with OSM2/EIRENE Scrape-Off Layer (SOL) density and temperature data. Numerous background parameters were varied to find the key mechanism behind the observed features in the heat deposition profiles. The SOL radial electric field emerges as the most likely cause for the peaking of the load profile near the separatrix on the outer target.

3.1 THE EFFECT OF VARIOUS PARAMETERS ON DIVERTOR LOADS

The ASCOT code was used in a scan of various parameters that may have a role in causing the observed features in JET divertor loads. First, in simple simulations searching for divertor target asymmetry trends caused by varying one parameter, ion ensembles of 1000 deuterons representing edge plasma ions in JET configuration (H-mode discharge #49511) were launched about 3 cm inside the separatrix ($\rho = 0{:}95$). Each particle was followed for 0.1 s or until it hit a divertor target. The particles experienced Coulomb collisions from a fixed JET background plasma inside the plasma and in the SOL. The results of a basic case in the normal and reversed magnetic field configuration indicate a strong asymmetry in the load distribution. Under normal configuration (with the ∇B drift downwards), the particle load of the inner target is much higher than that of the outer target. In the reversed magnetic configuration, the asymmetry is reversed.

This is, however, exactly opposite to the experimental observations which show a strong asymmetry in favour of the outer target when the ∇B drift is downwards [34]. It is therefore necessary to find and model the physical mechanism that is responsible for reversing the asymmetry.

In the initial ASCOT simulations, CX collisions were not modelled in the SOL. Experimentally, the neutral gas density is found to be higher in front of the inner target, thus possibly reducing the flux incident on the target. To take this into account, a model for SOL collisions was added to ASCOT. The collision model uses 2D background profiles obtained from the OSM2/

EIRENE code for electron, ion, and neutral density and temperature. Figure 3 shows the SOL atomic collisionality used in the ASCOT simulations. In addition to atomic collisions, which were found to be the dominant effect in the SOL, ion collisions were also modelled. Repeating the simulations with SOL collisionality lowered the overall target loads by about 60%, but did not change the load asymmetry towards the experimentally observed value (see Fig.4(a)). It was concluded that neutral collisions have little effect in this process.

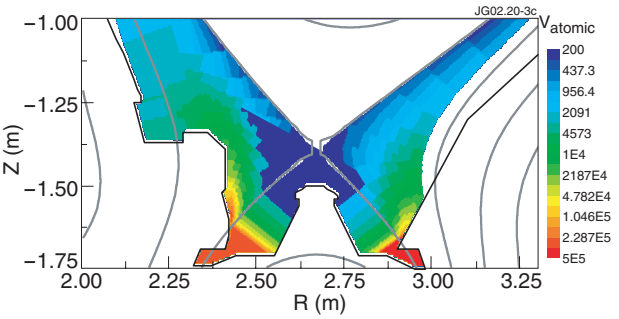

Fig.3: Atomic collisionality in the SOL as seen by ASCOT (only divertor region shown) based on JET discharge #49511. The data was obtained from the OSM2/EIRENE code.

Another factor possibly affecting the divertor load asymmetry is the radial electric field Er close to the separatrix inside the plasma. Simulations with different values of edge Er (ranging from -75 kV/m to +75 kV/m) were made using ASCOT. A negative edge Er substantially reduced the number of particles hitting the targets by squeezing their orbits thinner. The opposite phenomenon was seen for positive edge Er. However, the results (shown in Fig.4(b)) did not show any change in the target load asymmetry.

An obvious mechanism that could not only reverse the in-out asymmetry but also even strengthen the kinetic nature of the deposition profile is the radial electric field in the SOL. In a tokamak with the toroidal magnetic field pointing in the counterclockwise direction (as in the reference case), a positive Er (pointing radially outwards) provides the ions with a poloidal drift velocity favouring the outer divertor target. Indeed, as shown in Fig.4(c), the load asymmetry can be reversed by a positive SOL Er. This parameter was chosen for more detailed study.

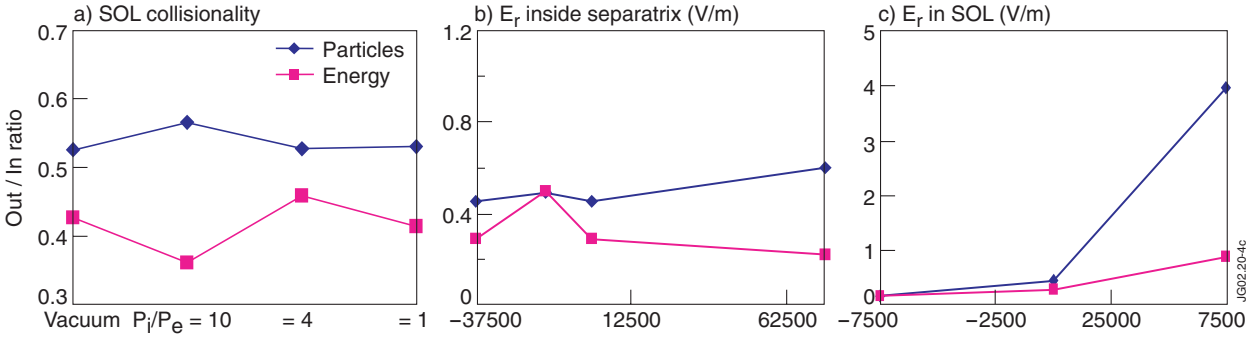

Fig. 4: Outer/inner target flux ratios for total ion flux (diamonds) and total heat flux (squares) (a) vs. SOL collisionality. (b) Vs. edge E_r inside the plasma. (c) Vs. SOL E_r.

To study the divertor target load profiles in detail, it is necessary to simulate the neoclassical steady-state situation in which any radial currents are balanced by an ambipolar radial electric field as described in Sec. 2. This method provides a steady-state density profile. Detailed self-consistent simulations with 420000 particles were made to obtain particle and energy deposition profiles on the targets. The SOL Er was assumed constant in the narrow region outside the separatrix which is

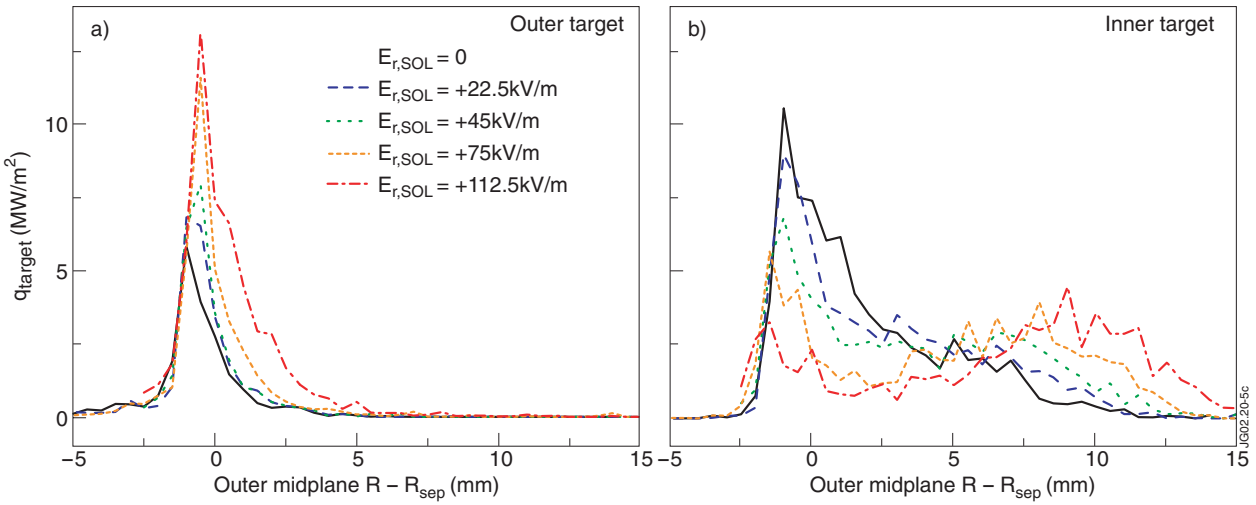

Fig. 5: ASCOT simulation of the effect of SOL E_r on power load pro¯les of outer and inner targets vs. the strike point magnetic surface distance from the separatrix along the outer midplane.

relevant to ions escaping from the plasma. The results, shown in Fig.5 as a function of R—R_{sep} (the distance [mm] of the strike point magnetic surface from the separatrix along the outer midplane), display a very narrow peak in the particle deposition pro¯le to the outer target. With increasing Er, the peak power at the outer target increases while the peak power to the inner target diminishes and the power is spread more evenly towards higher R—R_{sep} (upwards on the target). The cause for this is the Er x B drift, which points poloidally towards the outer target: ions moving towards the inner target have a smaller poloidal velocity, and thus the B x∇B drift has more time to displace them towards outer magnetic surfaces in the lower hemisphere. On the outer target, the opposite e®ect takes place. At large positive SOL Er values, the profiles as well as the target load asymmetry are in satisfactory agreement with measurements.

4. MOLECULAR DYNAMICS SIMULATIONS

The nature of plasma-wall interactions has recently been studied in detail using molecular dynamics simulations [35, 36, 37, 38, 39]. These simulations can both provide insight into the mechanisms of chemical and physical sputtering, as well as predict the sputtering yields of different hydrocarbons species separately.

In Molecular Dynamics (MD) simulations the motion of a system of atoms is followed by integrating Newton's equations of motion numerically [40]. The forces acting between the atoms and governing their motion are obtained either from classical interatomic potentials or quantum mechanical calculations.

The main source of uncertainty in MD simulations is the reliability of the force model used. For studies of plasma-wall interactions, one can use classical models or the simplest quantum mechanical model called "Tight Binding" (TB). More advanced models are too slow to study the dynamics of the interactions. The classical models of Brenner [41] and the TB model of the Frauenheim group [42] have been used here. Both models can describe carbon in the graphite, diamond and amorphous phases, as well as small hydrocarbon molecules and chemical reactions

between hydrogen, carbon and their molecules. They thus describe most of the features likely to be of importance when hydrogen coming in from a fusion plasma interacts with carbon-based wall materials.

The central results obtained to date in the MD simulation studies are presented here. The comparison of TB and classical results has shown that the central conclusions, first reached by classical methods, are valid also within a quantum mechanical picture [43]. The mechanism by which the chemical sputtering occurs has been demonstrated to be a "swift" chemical sputtering mechanism, which differs in nature from previously recognized chemical sputtering mechanisms. In it, an energetic hydrogen ion or neutral which enters the region between two carbon atoms can press the two atoms apart, breaking the chemical bond and causing sputtering [43]. The crucial difference to physical sputtering is that the threshold ion energy required for this process is the strength of the chemical bond, ~ 3 eV, as opposed to about 30eV for physical sputtering. This explains why carbon erosion is observed in reactors even at very low energies.

Another important observation is that the sputtering yields are extremely sensitive to the chemical environment in the first few atom layers facing the plasma. The sputtering yields for surfaces with a few dangling carbon molecules can exceed those for surfaces with only strongly bound carbons by an order of magnitude, even when the bulk chemical composition is the same. Similarly, at surfaces with a hydrogen coating produced by high H fluxes, the sputtering yields can drop by at least an order of magnitude [35]. This helps explain the large scatter between experimental results on carbon erosion yields obtained in different laboratories. It also clearly complicates quantitative prediction of sputtering yields; if the detailed surface composition in the reactor is not known, predicting yields without experimental input will be unreliable.

Nevertheless, the simulations can still be worthwhile, e.g., for predicting how much of the carbon is eroded for instance in CH_x vs. C_2H_x species, a quantity which is difficult to determine experimentally in reactor conditions. Results for such a prediction are given in Fig.6. It shows that except for the lowest-energy H ions, at least half of all carbon atoms are eroded in C_2H_x molecules

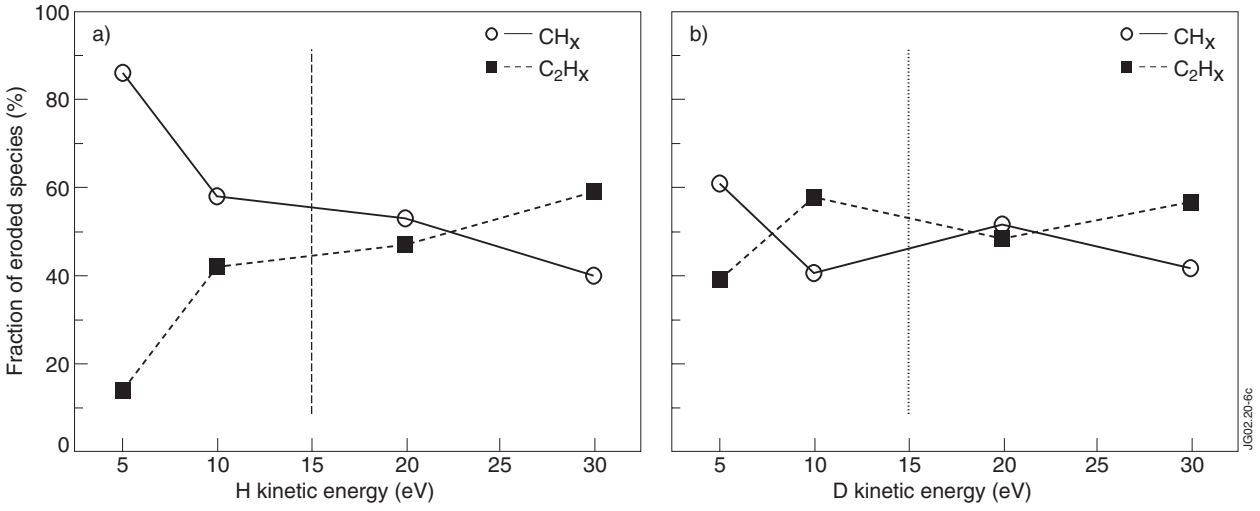

Fig.6: Fractions of sputtered small hydrocarbon molecules from a-C:H (left graph) and a-C:D (right graph) as a function of impinging H/D energy.

(note that the yield is not the carbon atom but molecule yield). If, for instance, the total carbon yield in the reactor is known, but not in which molecules they are sputtered away, information in this figure could be used to divide the total yield into molecular yields.

5. CONCLUSIONS

Validation of the orbit-following Monte Carlo method for studying various problems of edge plasma transport in fusion devices has been made. The effect of toroidal field ripple on CX diagnostics, the self-consistent calculation of the ambipolar radial electric¯eld, and the reproduction of experimentally observed divertor load profiles have been described. In addition to being applicable to self-consistent studies of edge plasma transport, the orbit-following Monte Carlo method allows flexible inclusion of realistic boundary conditions such as wall and divertor structures in the simulation, and is also well suited for simulating particle diagnostics.

Molecular dynamics simulations of plasma-wall interaction have been used in determining the sputtering yields of light hydrocarbons from amorphous carbon-hydrogen surfaces. With present-day computing power, such methods can be used to determine boundary conditions for edge plasma and neutral codes.

As the available computing power is rapidly and steadily increasing, a combination of the presented methods with Monte Carlo neutral codes may be used in the future for self-consistent edge plasma simulations, modelling the scrape-off layer and plasma-wall interactions in addition to the edge plasma and including the effects of turbulence.

ACKNOWLEDGEMENTS

This work has been carried out under the European Fusion Development Agreement.

REFERENCES

[1] Braams, B.J., Computational Studies in Tokamak Equilibrium and Transport, PhD Thesis, Utrecht University (1986)
[2] Schneider, R. et al., J. Nucl. Mater. 196-198(1992)810
[3] Simonini, R. et al., J. Nucl. Mater. 196-198(1992)369
[4] Rognlien, T.D. et al., J. Nucl. Mater. 196-198(1992)347
[5] Petravic, M., Phys. Plasmas 1(1994)2207
[6] Shimizu, K. et al., J. Nucl. Mater. 220-222(1995)410
[7 Reiter,D., Randschicht-Konfigurations von Tokamaks: Entwicklung und Anwendungstochastischer Modelle zur Beschreibung des Neutralgastransports, Rep. JUEL-1947, KFA Julich (1984).
[8] Stotler, D.P., Karney, C.F.F., Contrib. Plasma Phys. 34(1994)392; http://w3.pppl.gov/degas2/
[9] Cupini, E., De Matteis, A., Simonini, R., NIMBUS-Monte Carlo Simulation of Neutral Particle Transport in Fusion Devices, NET Rep. EUR XII-324/9 (1984).
[10] Rensink, M.E., Lodestro, L., Porter, G.D., et al., Contrib. Plasma Phys. 38(1998)325

[11] Thompson, M.W., Nucl. Instr. Methods Phys. res. B18(1987)411
[12] Post, D.E., J. Nucl. mater. 220-222(1995)143
[13] ITER Physics Basis: Power and Particle Control, Nuclear Fusion 39(1999)2931
[14] Lin, Z., Lee, W.W., Phys. Rev. E. 52(1995)5646
[15] Heikkinen, J.A. et al., "Particle Simulation of the Neoclassical Plasmas", to appear in Journal of Computational Physics
[16] Rognlien, T.D., Xu, X.Q., Cohen, R.H., Plasma Phys. Control. Fusion 42(2000)A271
[17] Scott, B., "Physics of Zonal Flows in Drift Wave Turbulence", in Theory of Fusion Plasmas, SIF, Bologna (2000)413
[18] Ma, S., Sydora, R.D., Dawson, J.M., Comput. Phys. Commun. 77(1993)190
[19] Kiviniemi, T.P., Heikkinen, J.A., Peeters, A.G., Nucl. Fusion 40(2000)1587
[20] Kiviniemi, T.P., Heikkinen, J.A., Peeters, A.G., Phys. Plasmas 7(2000)5255
[21] Kiviniemi, T.P. et al., Plasma Phys. Control. Fusion 43(2001)1103
[22] Heikkinen, J.A., Kiviniemi, T.P., Peeters, A.G., Phys. Rev. Lett. 84(2000)487
[23] Hahm, T.S., Burrell, K.H., Phys. Plasmas 2(1995)1648
[24] Heikkinen, J.A. et al., Phys. Plasmas 8(2001)2824
[25] Dumbrajs, O. et al., "Triggering Mechanisms for Transport Barriers", in 18th International Conference on Fusion Energy, Sorrento, Italia, October 4-10, 2000, Paper IAEA-CN-77/THP1/20, 6 pp.
[26] Kiviniemi, T.P., Heikkinen, J.A., Peeters, A.G., in this volume
[27] Herrmann, W. et al., Physical Review Letters 75(1995)4401
[28] Heikkinen, J.A. et al., Physics of Plasmas 4(1997)3655
[29] Heikkinen, J.A. et al., Physics of Plasmas 5(1998)692
[30] Sipila a, S.K. et al., Europhysics Conference Abstracts 24B(2000)1645
[31] Kurki-Suonio, T. et al., Plasma Physics and Controlled Fusion 42(2000)A277
[32] Kurki-Suonio, T. et al., EPS Conference Abstracts 24B(2001)1641-1644
[33] Kurki-Suonio, T. et al., in this volume
[34] Matthews, G.F. et al., J. Nucl. Mater. 290-293(2001)668
[35] Salonen, E. et al., Phys. Rev. B (Rapid Comm.) 60(1999)14005
[36] Salonen, E. et al., Europhys. Lett. 52(2000)504
[37] Salonen, E. et al., Phys. Rev. B 63(2001)195415
[38] Nordlund, K. et al., Nucl. Instr. Meth. Phys. Res. B 180(2000)77
[39] Salonen, E. et al., to appear in Applied Surface Science
[40] Allen, M.P., Tildesley, D.J., Computer Simulation of Liquids (Oxford University Press, Oxford, England, 1989)
[41] Brenner, D.W., Phys. Rev. B 42(1990)9458; idem, 46, 1948 (1992).
[42] Porezag, D. et al., Phys. Rev. B 51(1995)12947
[43] Krasheninnikov, A.V. et al., in this volume